Ingeniería Investigación y Tecnología
volumen XXVI (número 2), abril-junio 2025 1-11
ISSN 2594-0732 FI-UNAM artículo arbitrado
Información del artículo: Recibido: 10 de diciembre de 2024, aceptado: 11 de marzo de 2025

https://doi.org/10.22201/fi.25940732e.2025.26.2.014

Ingeniería Investigación y Tecnología

Finite element simulation of lateral wave propagation in an ultrasound transducer finding Crosstalk effect

Simulación por elementos finitos de la propagación de ondas laterales en un transductor de ultrasonido encontrando el efecto Crosstalk

Sánchez-Domínguez Israel (Corresponding autor)
Universidad Nacional Autónoma de México
Unidad Académica del Instituto de Investigaciones en Matemáticas Aplicadas y en Sistemas en el Estado de Yucatán
E-mail: israel.sanchez@iimas.unam.mx
https://orcid.org/0000-0002-7040-9552

Méndez-Monroy Paul Erick
Universidad Nacional Autónoma de México
Unidad Académica del Instituto de Investigaciones en Matemáticas Aplicadas y en Sistemas en el Estado de Yucatán
E-mail: erick.mendez@iimas.unam.mx
https://orcid.org/0000-0002-1726-6492

Bravo-Castillero Julian
Universidad Nacional Autónoma de México
Unidad Académica del Instituto de Investigaciones en Matemáticas Aplicadas y en Sistemas en el Estado de Yucatán
E-mail: julian@mym.iimas.unam.mx
https://orcid.org/0000-0002-7499-3821

Abstract

The reliable operation of an ultrasound transducer depends on the proper functioning of its piezoelectric elements. However, various factors can adversely affect its performance, particularly physical factors that compromise the transducer's structural integrity. One such factor is crosstalk, which induces spurious vibrations in the transducer elements. These unintended vibrations, generated by ultrasound waves, can gradually cause microstructural damage. This study introduces a novel approach by simulating the effects of crosstalk on the transducer's piezoelectric backing layer. Understanding these effects is crucial, as structural damage is often progressive and difficult to detect, potentially leading to failure or fracture of the backing layer. Analyzing the interaction between crosstalk and the transducer support can facilitate designs capable of minimizing damage caused by crosstalk. Additionally, collaboration with materials science and engineering fields can enhance the design and fabrication of more efficient and durable transducers.
Keywords: Matrix transducers, crosstalk, spurious vibrations, simulation.

Resumen

El desempeño confiable de un transductor de ultrasonido depende del correcto funcionamiento de sus elementos piezoeléctricos. Sin embargo, diversos factores pueden afectar negativamente su rendimiento, en particular, aquellos factores físicos que comprometen la integridad estructural del transductor. Uno de estos factores es la diafonía, que induce vibraciones espurias en los elementos del transductor. Estas vibraciones no deseadas, generadas por ondas ultrasónicas, pueden causar gradualmente daños microestructurales. Este estudio introduce un enfoque novedoso al simular los efectos de la diafonía en la capa de soporte del transductor piezoeléctrico. Comprender estos efectos es crucial, ya que el daño estructural suele ser progresivo y difícil de detectar, lo que puede llevar a la falla o fractura de la capa de soporte. Analizar la interacción entre la diafonía y el soporte del transductor, puede facilitar diseños capaces de minimizar los daños causados por la diafonía. Además, la colaboración con los campos de la ciencia de materiales e ingeniería puede mejorar el diseño y la fabricación de transductores más eficientes y duraderos.
Descriptores: Matriz de transductores, crosstalk (diafonía), vibraciones espurias, simulación.

Introduction

All ultrasound matrix transducers exhibit crosstalk, a phenomenon that arises from the interference and interaction of waves emitted and received by the piezoelectric elements within the transducer matrix. These interactions generate spurious waves originating from other elements of the transducer (Guess *et al.*, 1995; Dominguez *et al.*, 2011; Dominguez, 2015). During transducer operation, these spurious waves propagate in all directions through the piezoelectric elements of the matrix.

In transducer design, efforts are made to minimize wave transmission toward the rear of the device by incorporating a backing layer. This is particularly important when maximizing wave emission toward the front face is a priority.

However, lateral vibrations are of particular concern in this study, especially within the matrix of piezoelectric elements, where spurious waves emitted by all elements interact. Some of these waves collide with the matrix structure, leading to structural failures, particularly in the backing layer joints and the fasteners of the piezoelectric elements. Although these defects are on the micrometer scale, structural damage accumulates over time.

As a result, this progressive damage, combined with crosstalk, can cause a significant shift in the output frequency. Figure 1 illustrates an example of how lateral vibrations and spurious waves contribute to this damage.

This structural damage leads to attenuation, as well as alterations in the directivity pattern and power of the emitted beam, ultimately affecting the transducer's performance in various applications. In the medical field, for instance, beam precision is crucial for accurate diagnosis. Any errors caused by crosstalk can directly compromise the transducer's performance and reliability.

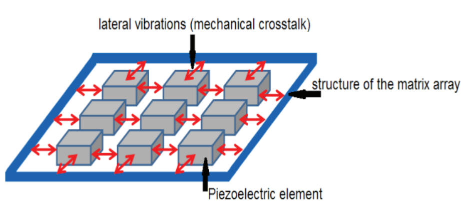

Figure 1. Illustration of mechanical crosstalk between piezoelectric elements in a matrix

The vibration of piezoelectric ceramics upon excitation is a natural mechanical effect. However, the spurious waves generated by this vibration must be minimized, as they can gradually cause structural damage and intensify the crosstalk phenomenon. Addressing this issue early in the transducer's life cycle is crucial, as structural damage, once present, leads to a further increase in crosstalk.

From a research perspective, this damage is significant, as it leads to a progressive decline in the transducer's performance. Various studies have proposed solutions to mitigate crosstalk, including the use of absorption materials or polymers (Zhou & Hossack, 2007; Yang, Cannata *et al.*, 2012). Another approach, particularly in medical equipment, involves correcting the ultrasound signal through electronic filters or signal processing techniques.

While these solutions can mitigate the issue, they do not address its root cause. Instead, they merely conceal the damage, delaying its detection and allowing further deterioration of the transducer matrix structure. Since spurious waves are inherently present during transducer operation, mechanical damage will inevitably accumulate, further amplifying the crosstalk phenomenon.

This study analyzes the crosstalk phenomenon in transducers, with a particular focus on its impact on the backing layer. The novelty of this work lies in the use of computer simulations to reveal crosstalk effects on the backing layer, a critical component in piezoelectric transducer design.

The significance of this research stems from the progressive nature of structural damage, which is often difficult to detect and may go unnoticed until a fracture occurs. By understanding the mechanisms of crosstalk and its effects on the backing layer, it becomes possible to develop more efficient transducers that minimize this theoretically observed damage.

Background

The interaction between mechanical and electrical effects in a linear piezoelectric element is analyzed using the finite element method (FEM). Key variables in this analysis include the second-rank tensor of mechanical stresses (σ), the second-rank tensor of mechanical strains (S), the electric field vector (E), the dielectric displacement vector (D), the fourth-rank mechanical stiffness tensor for a constant electric field (C^E), the second-rank permittivity tensor for constant mechanical strain (ε^S), and the third-order piezoelectric tensor (e) (Lerch, 1990).
Based on these variables, the constitutive equations for linear piezoelectric media can be expressed as follows:

$$\sigma = C^E S - e^T E \tag{1}$$

$$D = eS + \varepsilon^S E \tag{2}$$

Where the superscript T means transposed. The relevant geometrical equations that relate the mechanical strain S to the mechanical displacement vector u, and the electric field E with the electric potential θ are given by:

$$S = 1/2\ (\nabla u + \nabla u^T) \tag{3}$$

$$E = -\nabla\theta \tag{4}$$

Where the Nabla symbol is used to denote both the vector $\nabla\theta$ (the gradient of scalar field θ) and the tensor ∇u (the gradient of the vector field u) (Gurtin, 1981). The equation of motion for linear, force-free piezoelectric media is given by:

$$\nabla \cdot \sigma = \rho\, \frac{\partial^2 u}{\partial t^2} \tag{5}$$

Where $\nabla\sigma$ represents the unique vector field such that its scalar product with any vector a coincides with $\nabla\cdot(\sigma^T a)$ for every vector a, ρ denotes the mass density of the piezoelectric medium and t represents time. On the other hand, the electric behavior follows Maxwell's equation in the absence of volume charge:

$$\nabla \cdot D = 0 \tag{6}$$

Where $\nabla \cdot D$ represents the scalar field defined by the trace of the gradient of D, i.e. $tr(\nabla D)$. The Eq. 1 to Eq. 6 lead to a system of four partial differential equations for determining the displacement vector u and the electric potential θ. This problem can be computed by specifying appropriate boundary and initial conditions. Moreover, the elastic C^E, piezoelectric e and dielectric ε^s material functions satisfy the usual properties of symmetry and positivity, as outlined, for example, in the work of Akamatsu & Nakamura (2002).

Furthermore, in the case of composite materials, as illustrated in Figure 1, the equations must be satisfied in each of the regions occupied by the piezoelectric fibers and matrix. In such cases, interface conditions are required on the discontinuity surface between matrix and fibers.

In this work, we examine the continuity conditions for mechanical displacements, electric potential, and both mechanical and electrical fluxes, which are as follows:

$$[u] = 0,\ [\theta] = 0,\ [\sigma_n] = 0,\ [D_n] = 0 \tag{7}$$

Where $[x]$ denotes the jump in the function x at the interface, and n represents a unit normal vector to the discontinuity surfaces. Our objective is to utilize COMSOL software to obtain the solution using the finite element method (FEM).

The finite element discretization is performed by defining nodal solution variables and element shape functions over each finite element to approximate the solutions of Eq. 5 and Eq. 7, as described by Lerch (1990), as follows:

$$u_c = N_u^{\,T} \cdot u \quad \theta_c = N_\theta^{\,T} \cdot \theta \tag{8}$$

Where u_c and θ_c denote the displacement vector and the electric potential, respectively, within the finite element domain along the coordinate axes. N_u and N_θ represent the matrix of displacement shape functions and the vector of the electric potential, respectively. The application of Hamilton's variational principle in conjunction with the finite element discretization yields the following coupled finite element matrix equation:

$$\begin{bmatrix} M & 0 \\ 0 & 0 \end{bmatrix}\begin{bmatrix} \ddot{u} \\ \ddot{\theta} \end{bmatrix} + \begin{bmatrix} D_{uu} & 0 \\ 0 & 0 \end{bmatrix}\begin{bmatrix} \dot{u} \\ \dot{\theta} \end{bmatrix} + \begin{bmatrix} K_{uu} & K_{u\theta} \\ K_{u\theta}^T & K_{\theta\theta} \end{bmatrix}\begin{bmatrix} u \\ \theta \end{bmatrix} = \begin{bmatrix} F \\ Q \end{bmatrix} \tag{9}$$

Where:

$M = \int \rho N_u^{\,T} N_u dV$ = mass matrix
D_{uu} = mechanical damping matrix
$K_{uu} = \int S^T c^E S dV$ = mechanical stiffness matrix
$K_{u\theta} = \int S^T e^T \nabla\theta dV$ = piezoelectric coupling matrix
$K_{\theta\theta} = \int \nabla\theta^T \varepsilon^S \nabla\theta dV$ = dielectric stiffness matrix

Additionally, F denotes the structural load vector while Q represents the electrical load vector, both vectors include nodal, surface, and body charges. The integration is performed over the entire finite element domain. A detailed description of the derivation of Eq. 9 is provided in Lerch (1990). In practice, once these matrices have been generated and the finite element domain is specified, the software automatically recognizes all the parameters involved in Eq. 9 and proceeds with the finite element solution.

Methods, techniques, and instruments

In this study, the finite element method (FEM) is employed to design a structure organized as a square matrix, as depicted in Figure 2. The analysis focuses on structural damage and the propagation of a beam induced by spurious waves. The array comprises nine piezoelectric elements fabricated from PZT (Lead Zirconate Titanate) and operating at 8 MHz. These elements are constructed using commercial-grade PI ceramics (PI Ceramic GmbH, 1996) and are mounted on a polymer base analogous to that used in commercial transducers. The spacing between each ceramic element is one-quarter of the wavelength (1/4 λ), corresponding to 0.5 mm.

The complete array (comprising both the base and the piezoelectric elements) was built for experimental validation against simulated results. However, the present work focuses exclusively on the simulation of the array, and the comparison between experimental and simulated results is beyond its scope. The selection of a nine-element array was motivated by its simplicity in terms of physical construction and FEM design, and this configuration is widely adopted in commercial applications. For future research, we intend to investigate alternative geometric configurations and evaluate the effects of increasing the number of piezoelectric elements (Celmer & Opielinski, 2014).

In the finite element method (FEM) simulation, a free oscillation mode is considered, with the base of the piezoelectric ceramics fixed in place. This configuration is adopted because the base is bonded to the array structure, thereby enabling the observation of all interactions that occur when the elements are excited and interact with one another. Table 1 (Carrino *et al.*, 2018), presents the physical and mechanical properties of the piezoelectric ceramic employed in the FEM simulation (Berlincourt, 1971).

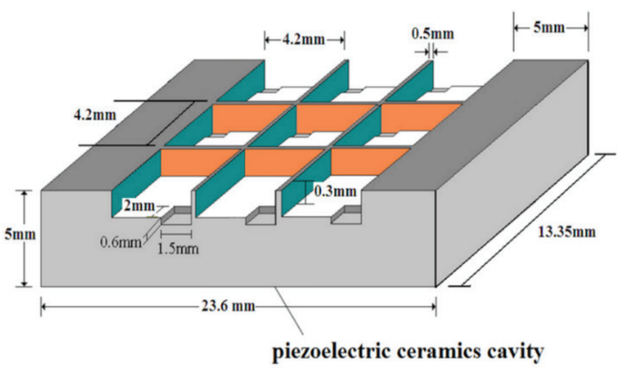

Figure 2. Structural design of the transducer array

To assess the influence of crosstalk within the matrix, the FEM results were analyzed in terms of frequency response. Additionally, the distribution of stress was evaluated to determine the mechanical stress imposed on the structure at critical points.

Table 1. Physical and mechanical properties of piezoelectric ceramic PIC255

Physical properties		
Density	$\rho[K_g/cm^3]$	7.8
Curie temperature	Tc[°C]	350
Permittivity -	$\varepsilon^T{}_{33}/\varepsilon_0$	1750
Permittivity ⊥	ε_ε	1650
Dielectric loss factor	Tanδ	20
Mechanical properties		
	K_p	0.62
	K_t	0.47
Coupling factor	K_{31}	0.35
	K_{33}	0.69
	K_{15}	0.66
	$d_{31}[(10^{-12}C/N)]$	–180
Piezoelectric charge constants	$d_{33}[(10^{-12}C/N)]$	400
	$d_{15}[(10^{-12}C/N)]$	550
Piezoelectric voltage constants	$g_{31}[(10^{-3}Vm/N)]$	–11.3
	$g_{33}[(10^{-3}Vm/N)]$	25

The tension observed in the structure may lead to structural failures. These failures are assumed to occur due to the influence of waves emitted by the piezoelectric elements, which induce sharp vibrations in the structure. Consequently, shearing forces develop, progressively increasing the level of damage. Figure 3 illustrates a typical failure in the array at critical points within the mechanical structure, where vibrations and stresses are most likely to cause structural degradation.

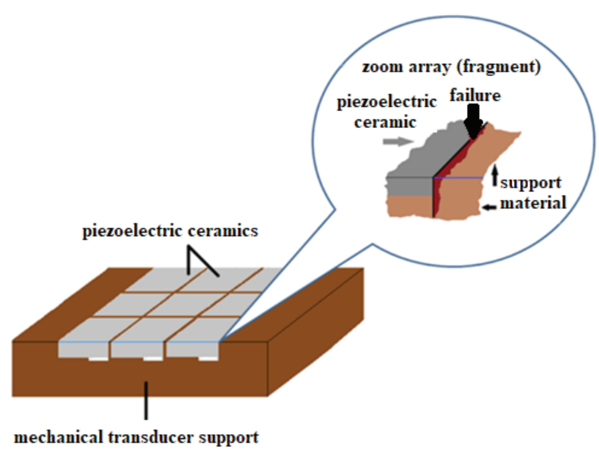

Figure 3. Example of a typical mechanical failure in the piezoelectric matrix when exposed to crosstalk waves

Results and discussion

The results of the simulation are presented below. In COMSOL software, key parameters such as frequency, the number of piezoelectric elements, Young's modulus, and the excitation area were considered. In this case, the excitation area was restricted to a hemisphere to simulate the radiation pattern.

Figure 4 illustrates the mesh used in the FEM simulations, highlighting the nine piezoelectric elements. The mesh is refined in regions where the elements are in close proximity, ensuring a more accurate solution and an improved design analysis. This refinement enhances the precision of the interactions between elements, leading to the vibration of all piezoelectric components and potentially causing structural failures within the matrix. The key parameters used in the simulation included a frequency of 8 MHz for each ceramic, the distance between the piezoelectric elements (as shown in Figure 2), and the mesh type with refinement in critical areas (as shown in Figure 3). Once these parameters were defined, an analysis range from 1 to 10 MHz was applied, along with the excitation signal illustrated in Figure 5. This stimulus initiates vibration in the ceramic elements.

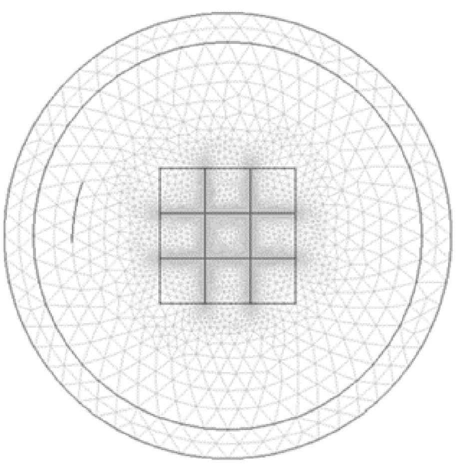

Figure 4. Finite element model of the analyzed PZT matrix

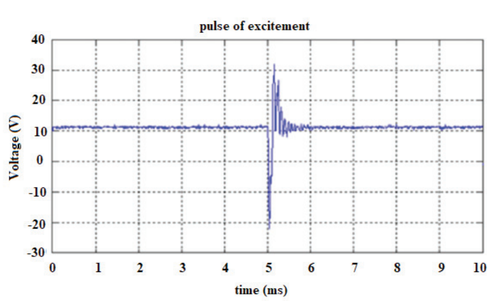

Figure 5. Excitation pulse used in the simulation

Figure 6 presents the resulting spurious vibrations in adjacent elements due to the excitation signal. These interactions lead to an increase in vibration modes, generating additional spurious vibrations. As shown in Figure 7, this vibration results in the formation of lobes extending in all directions of the piezoelectric ceramic.

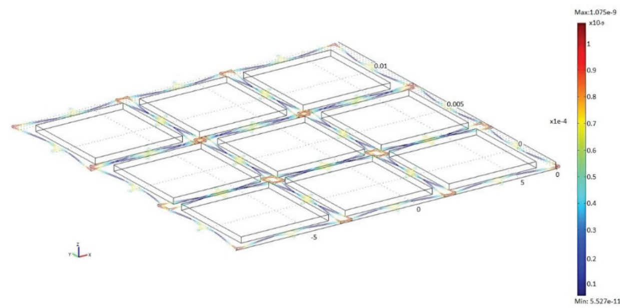

Figure 6. Initial vibration in piezoelectric elements: response obtained by FEM

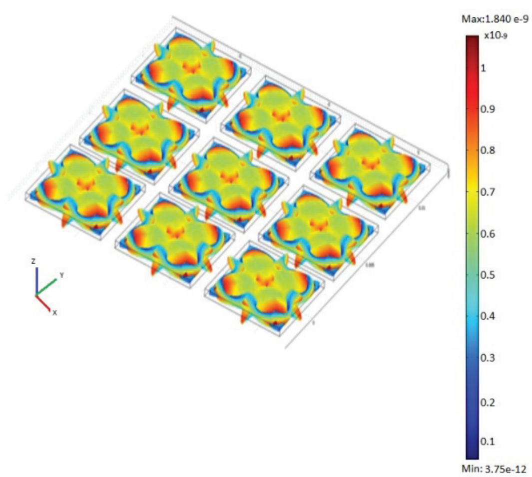

Figure 7. Oscillation of all piezoelectric elements with spurious vibrations

Figure 8 illustrates the response resulting from interactions between the generated spurious waves. As these interactions accumulate, the transducer response becomes increasingly chaotic, leading to performance degradation and distortion, including a frequency shift.

Figure 9 presents the deterioration of the vibration pattern as calculated by finite element analysis. The response begins to distort due to stimulation from other piezoelectric elements, with each element adjusting to the new excitation and interacting again. Over time, this continuous interaction alters the transducer's response, progressively affecting its physical structure.

Although this study did not primarily focus on the phenomenon of crosstalk, which is already well understood, its main objective was to examine the impact of spurious waves (generated by crosstalk) on the transducer structure and their propagation within it.

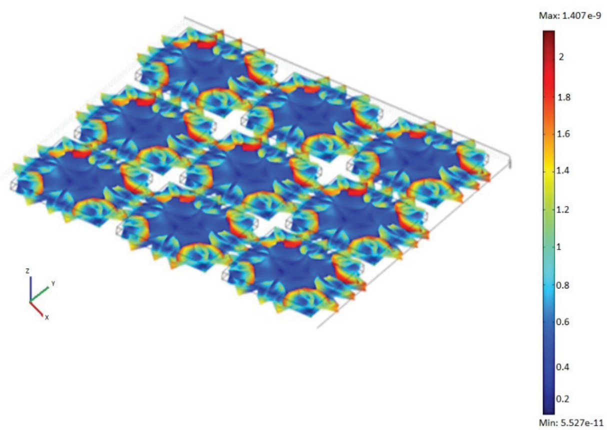

Figure 8. FEM Analysis of the response to stimuli from coupled piezoelectric elements

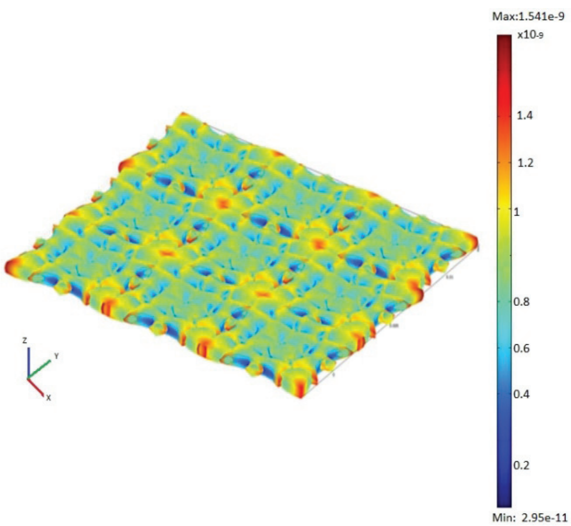

Figure 9. Over time, the interaction intensifies, leading to a progressive deterioration in the response

For this reason, the mechanical stress induced by the waves emitted toward the structure is analyzed. As shown in Figure 10, these waves propagate through the narrowest part of the structure, specifically the material separating the piezoelectric elements. A signal of considerable amplitude is observed, which has the potential to cause structural failure.

The magnified view in Figure 10 further illustrates how spurious vibrations gradually affect the transducer, leading to failures that intensify over time and ultimately compromise both the structure and performance of the transducer.

Figure 11 illustrates the propagation of spurious waves caused by the crosstalk phenomenon within the transducer structure. This figure emphasizes the early stages of failure, as the structure is primarily composed of polymer, which, due to its inherent physical properties, is not expected to exhibit substantial oscillations. Consequently, it is directly affected by the energy of the spurious waves, which act as constant impacts. Over time, these impacts weaken the support layer of the piezoelectric elements, creating air gaps between the structure and the elements, thereby disrupting the radiation pattern. Furthermore, these impacts diminish the mechanical integrity of the support layer, leading to fractures that propagate and, ultimately, result in the fragmentation of the structure. Such degradation can lead to the loss of piezoelectric elements, significantly diminishing the transducer's performance.

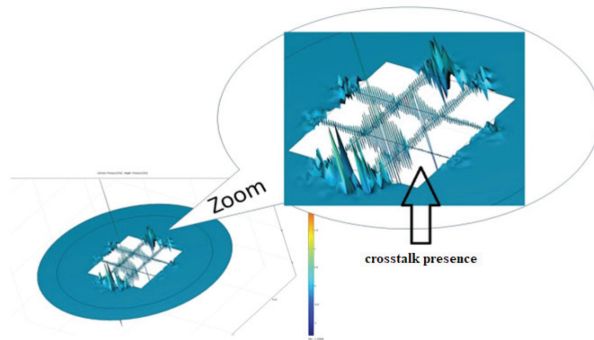

Figure 10. Waves that propagate through the structure causing structural failures, the detailed view shows more clearly than propagation

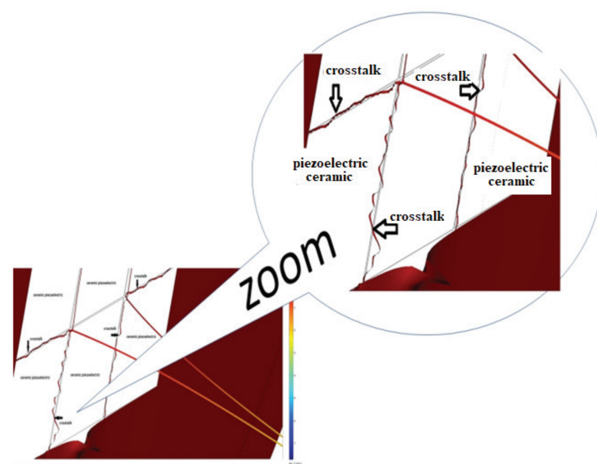

Figure 11. Spurious waves that propagate in the transducer structure, leaving visible the failure that occurs, the detailed view of the propagation of spurious waves allows to better observe said failure

Simulations conducted using FEM (illustrated in Figures 6 through 11) revealed the presence of crosstalk induced by lateral vibrations. The interaction between the crosstalk waves and the transducer structure was clearly observed, demonstrating how these interactions can potentially impact the transducer's performance. This observation prompted further investigation into whether the lateral vibrations were causing damage to the transducer. The simulations confirmed the interaction between the piezoelectric elements of the transducer, which gives rise to the crosstalk phenomenon.

This interaction amplifies crosstalk, leading to the generation of parasitic signals, which cause all elements to radiate these signals over time. Figure 12 shows both the main oscillation signal and the radiation of parasitic signals. These parasitic signals gradually induce a frequency shift in the main radiation signal, which may increase as time progresses.

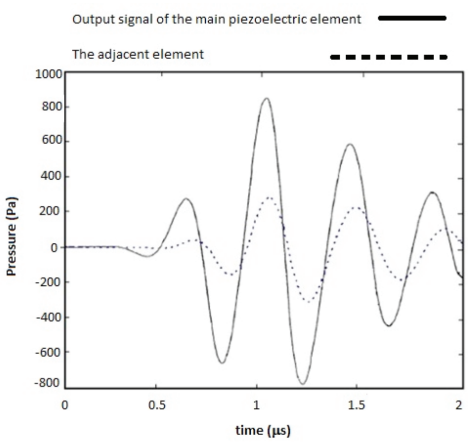

Figure 12. Signal emitted by the central piezoelectric element and the parasitic signals from each of the other piezoelectric elements over time

While finite element simulations are useful for suggesting the presence of the crosstalk phenomenon, they do not fully capture its impact on the transducer's performance. The effect on performance is most evident in the behavior of the main radiation lobe. According to theory (Israel, 2013), the main lobe will be affected in terms of amplitude, directionality, and operating frequency.

Over time, these interactions cause mechanical damage between the elements and their supports, potentially leading to destruction, fractures, or shear cracks within the array. The extent of this mechanical damage has not yet been quantitatively determined, as this analysis will be conducted in future work due to limitations in the physical construction of the array and the equipment required to quantify mechanical damage in the piezoelectric elements.

To investigate the impact of crosstalk on the radiation pattern, HP-Vee software (HPVEE, 2025), was used to simulate the behavior of the beam emitted by the transducer and its interaction with crosstalk. HP-Vee is a powerful visual programming environment that allows the development of programs by connecting graphical objects, rather than writing lines of code. The resulting programs resemble easy-to-understand block diagrams with connections between them (HPVEE, 2025).

Figure 13 illustrates a segment of the HP-Vee beam-crosstalk simulation, which incorporates key parameters that directly influence the transducer's performance, including frequency (f), the number of piezoelectric elements (N), the separation distance between the elements (d), and the crosstalk factor (α). These parameters interact with one another, enabling us to visualize the impact of crosstalk on the transducer's radiation pattern.

The simulation provided both visual and quantitative results, clearly demonstrating a direct relationship between the crosstalk caused by the lateral vibration modes and the emitted radiation pattern. This supports the hypothesis that structural damage in the transducer significantly impacts its performance.

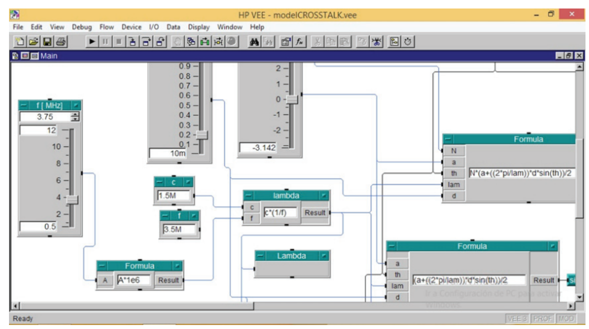

Figure 13. HP-Vee programming screen segment, used in beam-crosstalk simulation

The following graphs (Figure 14) illustrate how crosstalk increases and its effect on the radiation pattern:

- It can be observed that the frequency does not shift immediately. Instead, the shift begins once the elements of the matrix start to vibrate, and the lateral waves begin to interact with each other.
- When the crosstalk factor (α) exceeds a value of 2.5, the main lobe is accompanied by a lateral lobe of greater amplitude, which begins to compete with the main lobe (radiation pattern), as shown in graphs (g) and (h) of Figure 14.
- Mechanically, these oscillations (crosstalk) are one of the primary causes of damage to the structure, particularly to the backing layer of the piezoelectric elements.
- As shown in all the graphs, the frequency shift and the appearance of multiple lobes occur at high values of crosstalk, leading to degradation in the transducer›s performance.
- Additionally, it is evident that crosstalk directly affects the radiation pattern, causing the formation

https://doi.org/10.22201/fi.25940732e.2025.26.2.014

of additional lobes and a shift in the frequency of the resulting beam.

Table 2 displays the values obtained from the HPVee simulation, which were derived from the graphs shown in Figure 14. These values will be used to assess both the time and the extent of the damage caused to the structure.

Table 2. HP-Vee Simulation with 9 piezoelectri c elements and 0.2 mm separation

α (crosstalk)	**F [MHz]**	λ
0	5	0.3
0.5	5	0.3
1	4.93	0.3043
1.5	4.612	0.3252
2.5	4.557	0.3292
3.017	4.327	0.3467
3.127	4.098	0.366
3.141	3.969	0.3779

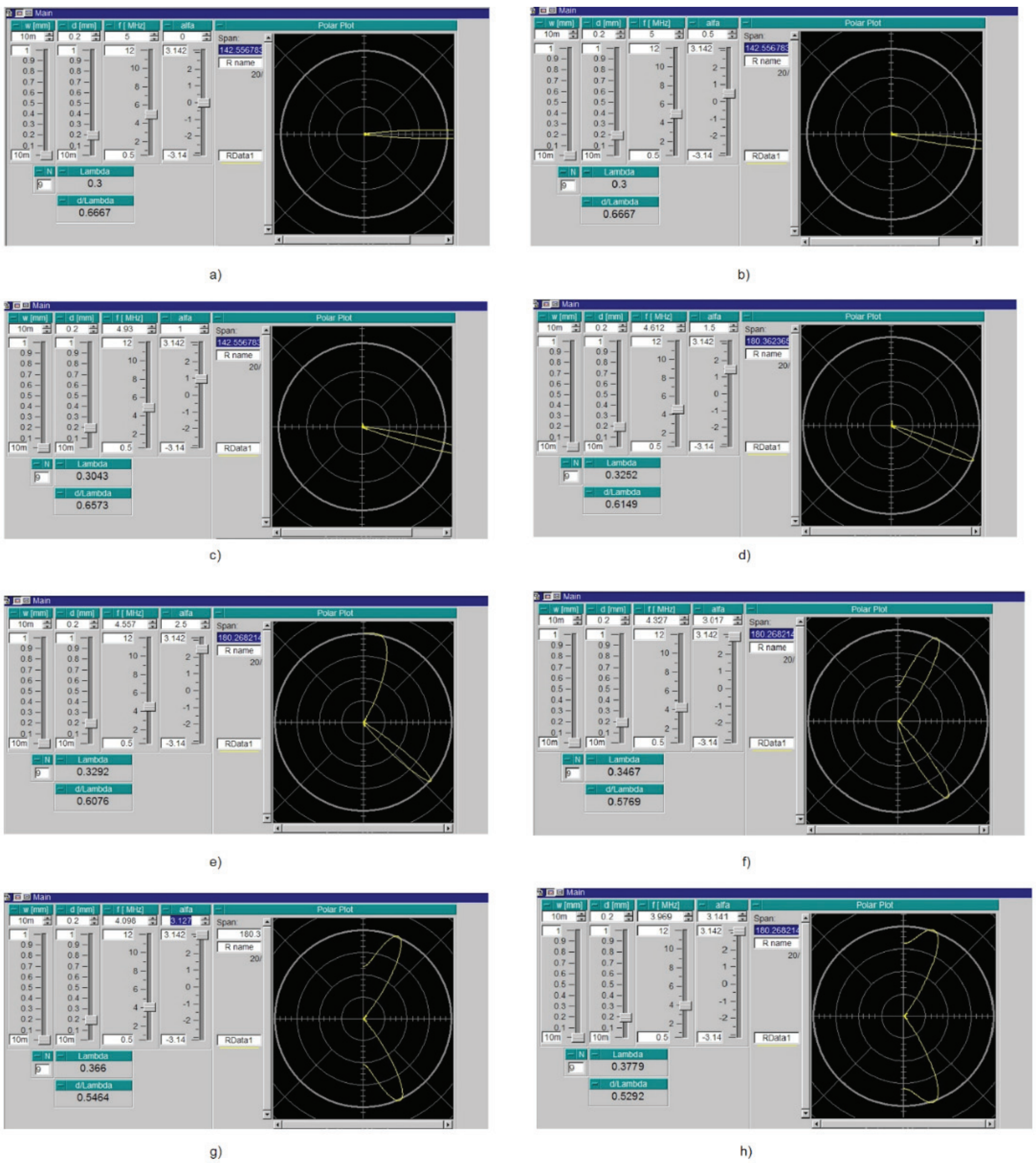

Figure 14. Representation of the results obtained from simulating crosstalk with HPVee. In each graph, it can be observed how increasing the degree of crosstalk modifies the resulting radiation pattern. In graph a), the response is shown with no crosstalk, and the crosstalk is progressively increased until graph h), where the radiation pattern is completely distorted

As observed, the less compressible the material (in this case, the backing layer of the piezoelectric elements), the faster sound is transmitted through it. Longitudinal mechanical waves propagate through the transmitting medium as oscillations, generating compression and rarefaction waves. Dense regions, where molecules are tightly packed, are referred to as compressions and correspond to areas of high pressure. Conversely, regions with fewer molecules are known as rarefactions and correspond to areas of low pressure. These compressions and rarefactions alternate throughout the medium, similar to how individual air particles oscillate back and forth in the direction of wave propagation.

Ultrasound transducers that use piezoelectric ceramics are generally expected to have a long service life. Although these ceramics age over time, their aging process typically follows a logarithmic pattern. For instance, a parameter such as transducer capacitance might change by 1 % from day 10 to day 100, and then by another 1 % from day 100 to day 1000, and so on. Most ultrasound equipment, including the transducers, typically has an average lifespan of approximately 10 years.

To explore ways to mitigate or reduce the degradation of the transducer structure, which can become fractured over time due to continuous exposure to ultrasound energy, it is important to consider the material's ability to absorb, attenuate, or divert this energy. When the structure cannot effectively manage these energies, it becomes vulnerable to damage. In this case, the material used for the transducer is Rexolite (Rexolite, 2025; Laminated Plastics Rexolite, 2017), a thermoset, rigid, and translucent plastic produced by crosslinking. One of Rexolite's key characteristics is its stable electrical properties. To assess the potential degradation caused by the impact of ultrasound waves, the acoustic impedance of Rexolite is examined. Acoustic impedance refers to the resistance a material offers to the propagation of sound, and it can be defined by the following equation:

$$Z = \rho \cdot \ \nu \tag{10}$$

Where:

ρ = density of the material and
ν = sound velocity

Considering the values for Rexolite (Laminated Plastics Rexolite, 2017), we have: $\rho = 1.05\ g/cm^3$, and $\nu = 236{,}220\ cm/s$. Substituting these values, we compute Z.

$$Z = (1.05)(236220) = 2.38031$$

Thus, Z is approximately 2.5 *Rayl*. From this, we can conclude that the less compressible the material, the faster the ultrasound is transmitted. Longitudinal mechanical waves propagate through the transmitting medium as back and forth oscillations, producing regions of compression and rarefaction. Acoustic impedance represents the ratio between the magnitude of a periodic action and the resulting response in the physical system (the transducer). It can be thought of as the ratio of waves propagating in a medium. This is represented by the following equation:

$$Z = P/\nu \tag{11}$$

Where ν is the speed of ultrasound and P is the sound pressure in the medium. Considering the associated values and substituting them into Eq. 11 with Z = 2.5 *Rayl* and ν = 2362.2 *m/s* and solving for the pressure P exerted on the material, we get:

$$P = Z \cdot \nu = (2.5)\ /2362.2) = 5905.5\ dB$$

The acoustic impedance, therefore, is a function that varies with frequency. A specific frequency (the frequency of oscillation) determinates the amount of pressure generated by the wave. For the transducer we need to determine the acoustic radiation impedance (Z_{ra}) (Soufflé, 2011). Acoustic impedance is particularly useful for this context and is given by:

$$Z_{ra} = Z/A \tag{12}$$

Where A represents the area of the vibrating surface, and in this case, A is computed with the dimensions presented in Figure 2. Similarly, we proceeded to substitute the values, which resulted in:

$$A = (0.3\ \text{mm}) \cdot (4.2\ \text{mm}) = 1.26\ \text{mm}^2$$

So, the acoustic radiation impedance (Z_{ra}) is calculated using the vibrating surface.

$$Z_{ra} = \frac{5905.5}{1.26} = 4686.91\,Rayls$$

This is interpreted as a significant amount of energy; however, it is also crucial to consider the duration of that energy. The literature generally defines the duration of an ultrasound pulse as ranging from 0.5 to 3 μs, with the total duration period spanning from 0.1 to 1 μs. (O'Brien, 2007). Assuming a year has 31,536,000 seconds, and considering that a transducer in medical applications is used at least 6 days a week such as in cardiology, gynecology, digestive system specialties, vascular surgery, neurology, urology, rheumatology, sports medicine, and other fields—ultrasound is typically applied for approximately 8 to 10 minutes per consultation (De, Fuente *et al.,* 2009; Díaz *et al.,* 2007). In perspective, although each pulse is brief, this prolonged exposure to ultrasound energy, combined with the mechanical stress exerted on the transducer, can gradually degrade its structure. Over time, this degradation may manifest as microfractures, material fatigue, or changes in acoustic properties, ultimately affecting the transducer's performance and lifespan.

Additionally, ultrasound in non-invasive imaging is widely used for diagnostic and therapeutic evaluations. For instance, hands-free 3D ultrasound is employed to monitor the portal vein, a crucial aspect of assessing liver and gastrointestinal function (Terada *et al.,* 2020). If the transducer sustains damage, it may lead to diagnostic errors, potentially resulting in severe and irreversible harm to patients. Therefore, the impact of Crosstalk-induced waves on transducer performance must be carefully considered. While further research is necessary, current findings suggest that Crosstalk does not directly deteriorate the piezoelectric ceramics, given their long lifespan. However, it compromises the supporting structure, which, over time, may indirectly lead to ceramic degradation.

In this study, FEM simulations were employed to analyze the effects of Crosstalk on the transducer structure. One potential cause of this issue is the inadequate attenuation capacity of the materials composing the structure, which fails to mitigate the impact of spurious waves. The simulations demonstrated that Crosstalk is amplified when lateral-mode vibrations occur in the piezoelectric elements. This intensified interaction between elements induces interference, ultimately diminishing the transducer's overall performance. As illustrated in Figure 11, spurious waves propagate through the transducer structure, and a detailed view highlights the structural failures resulting from this propagation.

Conclusions

This study conducted a comprehensive analysis of the nature and effects of the crosstalk phenomenon on the backing layer of a transducer. The findings confirm that crosstalk contributes to structural damage, which can be mitigated by incorporating absorption materials to reduce its impact. Since physical contact between the piezoelectric ceramics and the backing layer is unavoidable, optimizing material selection is essential. While the development of alternative materials and nanotechnology-based designs presents a promising avenue for improvement, further research is needed to explore their feasibility and effectiveness.

The findings of this study indicate that crosstalk, particularly at the outer perimeter of the piezoelectric ceramic interface, can cause significant interference among transducer elements. This interference is not merely an operational issue; simulation results that it may contribute to structural failures, especially in the backing layer. Over time, the cumulative effects of increased crosstalk and the absence of adequate absorption materials could lead to fractures, compromising the transducer's structural integrity and potentially rendering it non-functional.

Given these insights, further exploration of the mechanisms underlying crosstalk is essential to understanding its role in transducer performance degradation. While the FEM simulations provide a strong foundation for this hypothesis, empirical validation through experimental studies is necessary to confirm these findings. This study highlights the need for a more in-depth investigation into the crosstalk phenomenon, emphasizing the importance of developing a comprehensive methodology to quantify its effects and assess its destructive impact on the backing layers of transducers.

Future research should prioritize identifying effective strategies to mitigate crosstalk, potentially through the integration of targeted absorption materials, structural modifications or design enhancements that improve the transducer's overall resilience. Addressing these challenges will contribute to enhancing transducer reliability and performance, thereby advancing the field of piezoelectric devices.

Acknowledgments

We extend our gratitude to IIMAS-UNAM for its support and to Joaquin Morales for the technical assistance. This work was partially supported by UNAM-PAPIIT IN101822 and UNAM-PAPIIT IN105623.

References

Akamatsu, M., & Nakamura, G. (2002). Well-posedness of initial-boundary value problems for piezoelectric equations. *Applicable Analysis*, 81(1), 129-141. https://doi.org/10.1080/0003681021000021105

Berlincourt, D. (1971). *Piezoelectric crystals and ceramics*. Boston, MA: Springer. Pp. 129-141.

Carrino S., Nicassio F., & Scarcelli G. (2018). Nonlinearities associated with impaired sensors in a typical shm experimental Set-Up. *MDPI Electronics*, 7(11), 303. https://dx.doi.org/10.3390/electronics7110303

Celmer, M., & Opielinski, K. J. (2014). Crosstalk effects in multielement ultrasonic transducer arrays. On: Proceedings of the European Acoustics Association, 7. (the Forum Acusticum, Krakow, Poland). Retrieved on https://doi.org/10.7307/ptt.v27i1.1773

De, R., Fuente, S., Altermatt, F., & Corvetto, M. (2009). Conceptos básicos de ultrasonografía aplicada a la anestesia regional. *Rev Chil Anest*, 38, 40-46. https://revistachilenadeanestesia.cl/PII/revchilanestv38n01.07.pdf

Díaz-Rodríguez, N., Garrido-Chamorro, R., & Castellano-Alarcon, J. (2007). Ecografía: principios físicos, ecógrafos y lenguaje ecográfico. *SEMERGEN-Medicina de Familia,* 33(7), 362-369. https://doi.org/10.1016/S1138-3593(07)73916-3

Dominguez, I. S. (2015). Crosstalk in ultrasonic transducers, a first look. *IEEE Latin America Transactions*, 13(3), 589-598. https://doi.org/10.1109/TLA.2015.7069079

Dominguez, I. S., Contla, P. A., Hernandez, E. M., & von Kruger, M. A. (2011). Crosstalk efects caused by the geometry of piezoelectric elements in matrix ultrasonic transducers. *Brazilian Journal of Biomedical Engineering*, 27, 90-97. http://dx.doi.org/10.4322/rbeb.2011.008

Guess, F., Oakley, C. C., Douglas, S. J., & Morgan, R. D. (1995). Cross-talk paths in array transducers. On: Proceedings of the IEEE ultrasonics symposium, 1279-1282. Retrieved march 2025 on https://doi.org/10.1109/ULTSYM.1995.495790

Gurtin, M. E. (1981). *An introduction to continuum mechanics.* New York: Academic Press INC.

HPVEE (2025). (Visual Engineering Environment) HPE2120C Technical Specifications. Retrieved march 2025 on https://www.electronicsdatasheets.com/download/108748.pdf?format=pdf

Israel, S.-D. (2013). *Efecto del cross-talk en la respuesta de un transductor ultrasónico tipo pzt*. (tesis phd). Universidad Politécnica de Madrid, España. Retrieved on https://doi.org/10.20868/UPM.thesis.23319

Laminated Plastics Rexolite (2017). Technical data sheet rexolite. Computer software manual. Retrieved on https://laminated-plastics.com/rexolite.pdf

Lerch, R. (1990). Simulation of piezoelectric devices by two- and three-dimensional finite elements. *IEEE Transactions on Ultrasonics Ferroelectric and Frequency Control*, 37(2), 233-247. https://doi.org/10.1109/58.55314

O'Brien, W. D. (2007). Ultrasound–biophysics mechanisms. *Progress in Biophysics and Molecular Biology*, 93(1-3), 212-255. https://doi.org/10.1016/j.pbiomolbio.2006.07.010

PI Ceramic technology GmbH. (1996). Computer software manual. Fundamentals. Retrieved on https://www.piceramic.com/en/expertise/piezo-technology/fundamentals

Rexolite (Polymer plastics). (2025). Retrieved march 2025 on https://www.polymerplastics.com/rexolite-high-performance-plastic.shtml

Soufflé-Carvajal, F. J. (2011). *Resonancias de Helmholtz.* (Bachelors Thesis). Universidad de Sonora. Retrieved on http://www.bidi.uson.mx/TesisIndice.aspx?tesis=21819

Terada, I., Togoe, Y., Teratoko, T., Ueno, T., Ishizu, K., Fujii, Y., Sugimoto, N. (2020). Monitoring of portal vein by three-dimensional ultrasound image tracking and registration: toward hands-free monitoring of internal organs. *Advanced Biomedical Engineering*, 9, 1-9. https://doi.org/10.14326/abe.9.1

Yang, H.-C., Cannata, J., Williams, J., & Shung, K. K. (2012). Crosstalk reduction for highfrequency linear-array ultrasound transducers using 13 piezo-composites with pseudo random pillars. *IEEE Transactions on Ultrasonics, Ferroelectrics, and Frequency Control*, 59, 2312-2321. https://doi.org/10.1109/TUFFC.2012.2456

Zhou, S., & Hossack, J. A. (2007). Reducing inter-element acoustic crosstalk in capacitive micromachined ultrasound transducers. *IEEE Transactions on Ultrasonics, Ferroelectrics, and Frequency Control,* 54, 1217-1228. https://doi.org/10.1109/TUFFC.2007.375

Cómo citar:

Sánchez-Domínguez, I., Méndez-Monroy, P. E., & Bravo-Castillero, J. (2025). Finite element simulation of lateral wave propagation in an ultrasound transducer finding Crosstalk effect. *Ingeniería Investigación y Tecnología,* 26(02), 1-11. https://doi.org/10.22201/fi.25940732e.2025.26.2.014